

Magnetic catalysis in weakly interacting hyperbolic Dirac materials

Noble Gluscevic^{1,2} and Bitan Roy^{2,*}

¹*Department of Physics and Astronomy, Louisiana State University, Baton Rouge, LA 70803, USA*

²*Department of Physics, Lehigh University, Bethlehem, Pennsylvania, 18015, USA*

(Dated: May 19, 2023)

Due to linearly vanishing density of states, emergent massless Dirac quasiparticle resulting from the free fermion motion on a family of two-dimensional half-filled bipartite hyperbolic lattices feature dynamic mass generation through quantum phase transitions only for sufficiently strong finite-range Coulomb repulsion. As such, strong nearest-neighbor Coulomb repulsion (V) is conducive to the nucleation of a charge-density-wave (CDW) order with a staggered pattern of average fermionic density between two sublattices of bipartite hyperbolic lattices. Considering a collection of spinless fermions (for simplicity), here we show that application of strong external magnetic fields by virtue of producing a *finite* density of states near the zero energy triggers the condensation of the CDW order even for *infinitesimal* V . The proposed magnetic catalysis mechanism is operative for uniform as well as inhomogeneous (bell-shaped) magnetic fields. We present scaling of the CDW order with the total flux enclosed by hyperbolic Dirac materials for a wide range of (especially subcritical) V .

Introduction. Massless Dirac fermions living above one spatial dimension feature vanishing density of states (DOS). As a result, dynamic mass generation through the spontaneous breaking of any discrete and/or continuous symmetry (Anderson-Higgs mechanism) in Dirac materials only occurs at strong coupling via quantum phase transitions, typically triggered by the finite range components of Coulomb repulsion [1–4]. Crystalline symmetry protection of the Dirac points in the Brillouin zone, where the filled valence and empty conduction bands touch each other, severely restricts the number of Euclidean lattices on which free-fermions motion gives birth to massless Dirac quasiparticles. Graphene’s honeycomb [5] and π -flux square [6] lattices are the lone members of this family.

Negatively curved hyperbolic quantum crystals, in this respect opens a new direction. Throughout we characterize two-dimensional hyperbolic (and Euclidean) lattices, realized by repeated arrangements of polygons with p arms of equal length (p -gon), each vertex of which is accompanied by q equidistant nearest-neighbor (NN) sites, by a pair of integers (p, q) (Schläfli symbol). Then, a honeycomb [square] lattice is denoted by $(6, 3)$ [(4, 4)]. The geometric diversity of the hyperbolic lattices, stemming from the inequality $(p - 2)(q - 2) > 4$, gives rise to a variety of electronic band structures, captured by simple NN tight-binding model for free fermions [7–15]. In particular, a family of hyperbolic lattices with $q = 3$ harbors emergent massless Dirac fermions near the half-filling, when $p/2$ is an odd integer [15], hereafter named hyperbolic Dirac materials (HDMs). All hyperbolic lattices with odd $p/2$ is bipartite in nature, as then the NN sites belong to two sublattices, A and B (say). See Fig. 1.

HDMs constitute an ideal platform to explore (theoretically and possibly experimentally) novel effects of electronic interactions among massless Dirac fermions living on a curved space. For example, strong NN Coulomb (V)

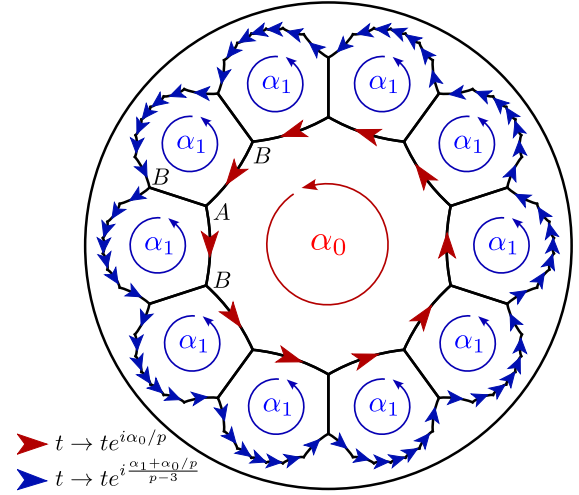


FIG. 1. Magnetic flux attachment to a $(10, 3)$ hyperbolic lattice through the Peierls substitution. The black lines represent a real and uniform hopping amplitude t between the nearest-neighbor (NN) sites, belonging to the A and B sublattices. When accompanied by the red or blue arrows the NN hopping amplitude becomes complex in its direction with the phases shown in the legend. Then α_0 (α_1) amount of magnetic flux pierces through the plaquette(s) belonging to the zeroth (first) generation. This construction can be generalized to mimic arbitrary flux profile to arbitrary generation on any hyperbolic lattice. Throughout we measure the magnetic flux in units of $\Phi_0/(2\pi)$, where $\Phi_0 = h/e$ is the flux quantum.

and on-site Hubbard (U) repulsions support sublattice symmetry breaking charge-density-wave (CDW) and antiferromagnetic orders, respectively, displaying staggered pattern of electronic density and magnetization between two sublattices. Furthermore, with increasing curvature or p , the critical strengths of V and U for these two orderings decrease monotonically, which are also smaller than

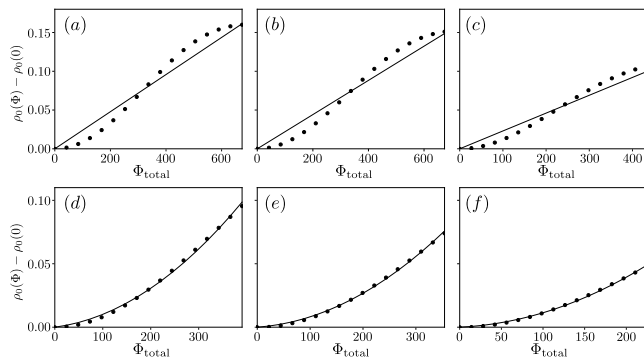


FIG. 2. Scaling of the density of states (DOS) near the zero energy $\rho(0) = \rho_0(\Phi) - \rho_0(0)$, where $\rho_0(\Phi) [\rho_0(0)]$ is the DOS with (without) magnetic field, with the total flux (Φ_{total}) enclosed by (10,3) [(a) and (d)], (14,3) [(b) and (e)] and (18,3) [(c) and (f)] hyperbolic lattices in the presence of uniform [(a)-(c)] and bell-shaped inhomogeneous [(d)-(f)] magnetic fields. For details see ‘Magnetic flux profiles’. We subtract $\rho_0(0)$ to remove finite size and DOS smoothing effects.

their counterparts on a relativistic flatland (honeycomb lattice) [15]. While this observation strongly suggests a fascinating phenomenon: Curvature induced quantum phase transition at weak coupling, no ordering develops for infinitesimal interactions in HDMs, due to the linearly *vanishing* DOS near the half-filling.

Key results. We show that the application of strong magnetic fields [Fig. 1] in HDMs creates a *finite* DOS near the zero energy or half-filling [Fig. 2]. Consequently, a sufficiently weak or subcritical NN Coulomb repulsion then nucleates a CDW order in these systems, a mechanism known as *magnetic catalysis* [16–22]. These outcomes hold for a uniform as well as a bell-shaped inhomogeneous magnetic field for which the field strength decreases monotonically from the center of the system toward its boundary [Fig. 3]. Formation of the CDW order splits the zero energy manifold and gives rise to a correlated insulator at half-filling [Fig. 4]. We arrive at these conclusions from numerical self-consistent solutions of the CDW order on (10,3), (14,3) and (18,3) HDMs with open boundary condition in the presence of uniform and inhomogeneous magnetic fields for a wide range of subcritical NN Coulomb repulsion within the Hartree-Fock or mean-field approximation. Throughout we consider a collection of spinless fermions for simplicity.

Magnetic flux profile. At first, we outline the details of the systems and the magnetic flux profiles considered in this work. All the numerical analyses are performed on a third generation (10,3), and second generation (14,3) and (18,3) hyperbolic lattices, respectively containing 2880 (421), 1694 (155) and 4050 (271) lattice sites (p -gons or plaquettes). The center plaquette corresponds to the zeroth generation and each successive layers of plaquettes constitute progressively next generations of the hyper-

bolic lattice. When the field is uniform, equal flux (α_0) threads all the plaquettes. A bell-shaped inhomogeneous magnetic field is modeled by threading α_0 , $0.85\alpha_0$, $0.70\alpha_0$ and $0.55\alpha_0$ amount of magnetic flux through all the plaquettes belonging to the zeroth, first, second and third generation of the (10,3) hyperbolic lattice, respectively. On (14,3) and (18,3) hyperbolic lattices then α_0 , $0.75\alpha_0$ and $0.50\alpha_0$ magnetic flux pierces through each plaquette belonging to the zeroth, first and second generation, respectively. We measure the magnetic flux in units of $\Phi_0/(2\pi)$, where $\Phi_0 = h/e$ is the magnetic flux quantum.

Free fermions. We begin the discussion with a tight-binding Hamiltonian for free fermions (H_0), allowed to hop only between the NN sites of the hyperbolic lattices, subject to magnetic fields. For spinless fermions, only the orbital effect of the external magnetic field is pertinent, captured by the Peierls substitution [23]. Then

$$H_0 = - \sum_{j \in A} \sum_{k \in B} ' t_{jk} c_j^\dagger \exp[i\alpha_{jk}] c_k + H.c, \quad (1)$$

where $i = \sqrt{-1}$, c_j^\dagger (c_j) is the fermionic creation (annihilation) operator on the j th site and the prime symbol restricts the summation within the NN sites. The sublattice labeling of the sites is arbitrary, manifesting an Isinglike sublattice exchange symmetry. The spin independent NN hopping amplitude t_{jk} is assumed to be constant t , which we set to be unity. As shown in Fig. 1, this prescription can be employed on any hyperbolic lattice to mimic any spatial profile of the magnetic field. As such uniform magnetic fields can display many peculiar phenomena on hyperbolic lattices [24–28], such as the Hofstadter butterfly, devoid of fractal structures [27].

We focus near the zero energy of half-filled HDMs, subject to magnetic fields. They possess a particle-hole symmetry about the zero energy and keep all the negative (positive) energy states occupied (empty). The average fermionic density at each site is then 1/2, manifesting the sublattice exchange symmetry. In Euclidean Dirac systems, application of external magnetic fields produces zero energy states, the number of which is proportional to the total magnetic flux enclosed by the system (Φ_{total}), irrespective of the magnetic field profile: Aharonov-Casher index theorem [29]. It has been verified from honeycomb lattice-based exact numerical diagonalization [21] and possibly also extends to HDMs [30, 31].

Here we compute the DOS near the zero energy $\rho(0)$ from exact numerical diagonalization of H_0 [Eq. (1)]. See Fig. 2. When the field is uniform, $\rho(0)$ scales *almost* linearly with Φ_{total} over its large range. The absence of infinitely degenerate zeroth and other Landau levels in HDMs roots in their nontrivial spatial curvature. In the small flux regime $\rho(0)$ scales *quadratically* with Φ_{total} for both uniform and bell-shaped inhomogeneous magnetic fields. These observations qualitatively conform to the Aharonov-Casher index theorem, extended to HDMs,

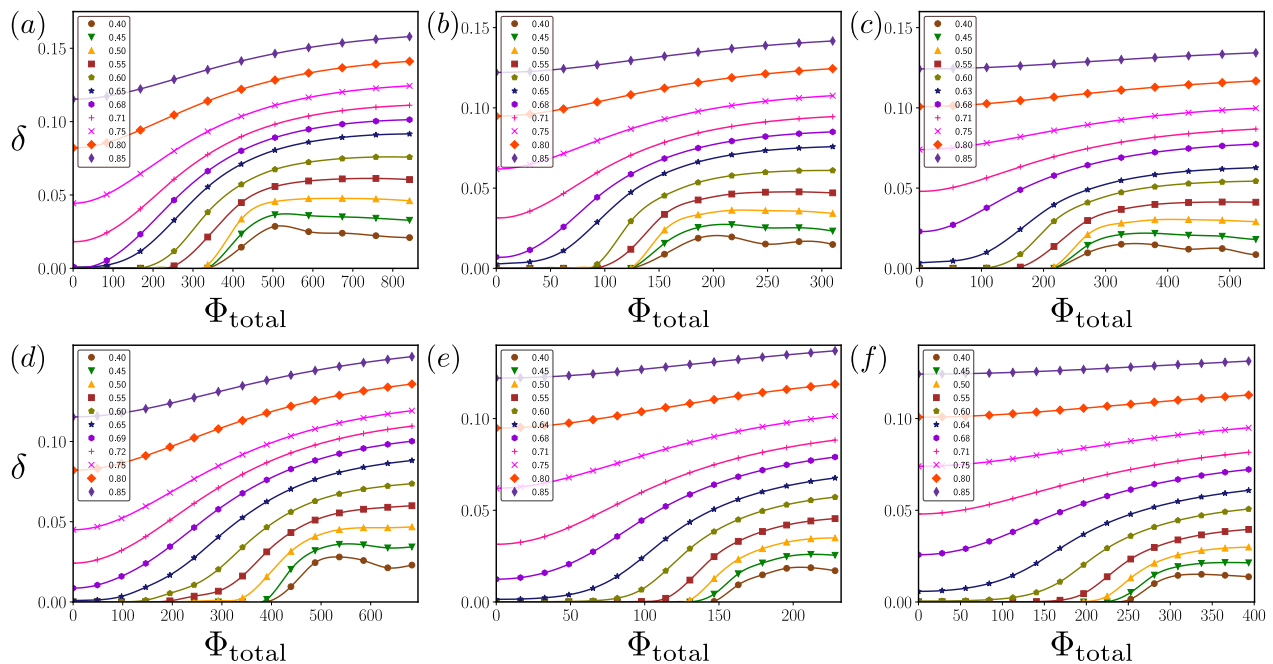


FIG. 3. Scaling of the charge-density-wave (CDW) order parameter δ [Eq. (4)], computed over the entire (10,3) [(a) and (d)], (14,3) [(b) and (e)] and (18,3) [(c) and (f)] hyperbolic lattices with open boundary condition in the presence of uniform [(a)-(c)] and bell-shaped inhomogeneous [(d)-(f)] magnetic fields, with the total magnetic flux enclosed by the system Φ_{total} for a wide range of the nearest-neighbor (NN) Coulomb repulsion (V) among spinless fermions. For details see ‘Magnetic flux profiles’. The zero magnetic field critical NN Coulomb repulsion for the CDW ordering is $V_c \approx 0.69, 0.67$ and 0.66 in (10,4), (14,3) and (18,3) hyperbolic lattices, respectively [15]. Therefore, application of strong magnetic fields by virtue of developing a finite DOS near the zero energy [Fig. 2] catalyzes the formation of the CDW order for sufficiently weak NN Coulomb repulsion ($V \ll V_c$), yielding a correlated insulator near the half-filling [Fig. 4].

possibly indicating a topological protection of the field induced near zero energy modes. Most crucially, when immersed in magnetic fields HDMs always supports finite DOS near zero energy. It can be conducive to the nucleation of ordered phases even for sufficiently weak finite-range Coulomb repulsion, which we discuss next.

NN repulsion. The zero energy manifold in HDMs induced by the external magnetic field, featuring a finite DOS, can be split by weak enough NN Coulomb repulsion (V) through a dynamic breaking of the sublattice exchange symmetry. For a collection of N spinless fermions, the corresponding Hamiltonian reads as

$$H_V = H_0 + \frac{V}{2} \sum_{\langle j,k \rangle} n_j n_k - \mu N. \quad (2)$$

Here $n_j = c_j^\dagger c_j$ is the fermionic density on site j , μ is the chemical potential in half-filled system, and $\langle \dots \rangle$ restricts the summation to the NN sites. A Hartree decomposition of the quartic term then leads to the following effective single-particle Hamiltonian [21, 32, 33]

$$H_V^{\text{Har}} = H_0 + V \sum_{\langle j,k \rangle} \left[\langle n_{A,j} \rangle n_{B,k} + \langle n_{B,j} \rangle n_{A,k} \right] - \mu N, \quad (3)$$

where $\langle n_A \rangle$ ($\langle n_B \rangle$) corresponds to the site dependent self-consistent average fermionic density on the sublattice A (B). We measure them relative to the uniform density at half-filling according to $\langle n_{A,j} \rangle = 1/2 + \delta_{A,j}$ and $\langle n_{B,j} \rangle = 1/2 - \delta_{B,j}$. To maintain the system at the half-filling, we choose $\mu = V/2$ and ensure that $\sum_j (\delta_{A,j} - \delta_{B,j}) = 0$. The positive definite quantities δ_A and δ_B yield the CDW order parameter in the whole system, defined as

$$\delta = \frac{1}{2} \left(\sum_j \delta_{A,j} + \sum_j \delta_{B,j} \right). \quad (4)$$

We numerically compute $\delta_{A,j}$ and $\delta_{B,j}$, and subsequently δ in the entire system with open boundary condition for a wide range of V , especially for its subcritical strengths, in the presence of uniform and inhomogeneous magnetic fields of varying Φ_{total} . For details consult ‘Magnetic flux profile’. The results are shown in Fig. 3.

Magnetic catalysis of CDW. The zero magnetic field critical strengths of the NN Coulomb repulsion for the CDW ordering are respectively $V_c = 0.69, 0.67$ and 0.66 in (10,3), (14,3) and (18,3) hyperbolic lattices of the specified generation number [see ‘Magnetic flux profile’] [15]. As shown in Fig. 3, in the presence of finite magnetic flux δ_A and δ_B , and concomitantly δ becomes finite in the entire system even when $V \ll V_c$ in these three HDMs.

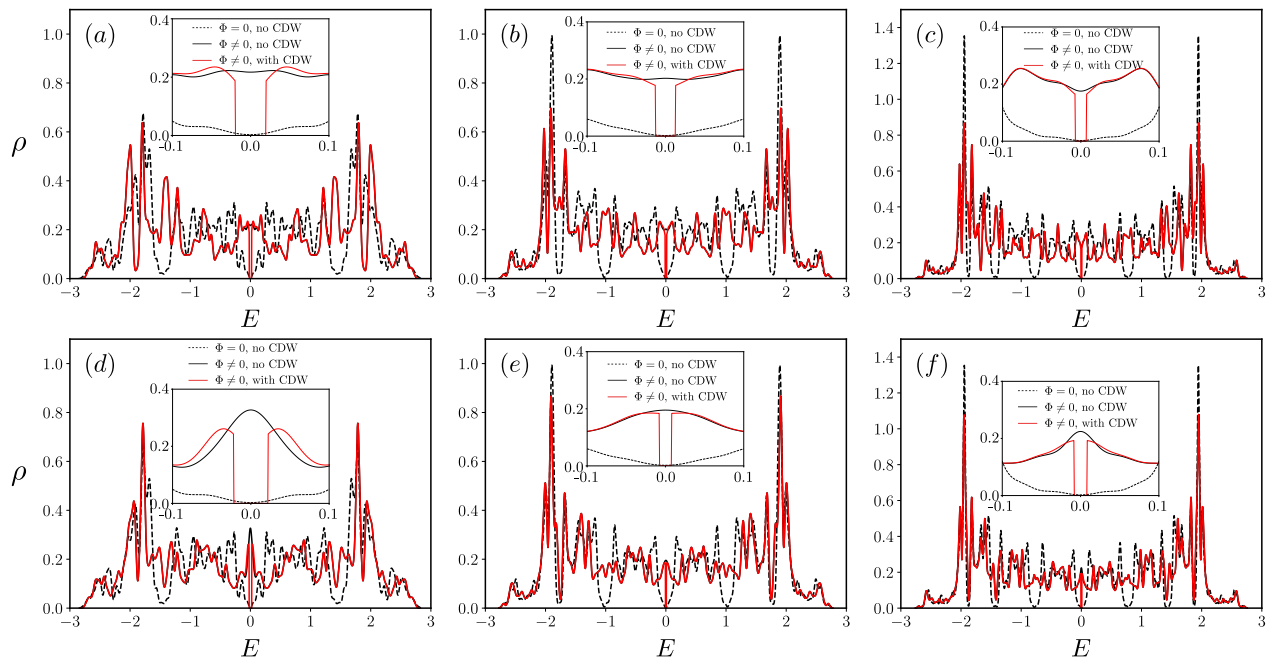


FIG. 4. Energy (E) vs density of states (ρ) in the absence (black dashed lines) and presence (black solid lines) of magnetic flux without the charge-density-wave order in (10,3) [(a) and (d)], (14,3) [(b) and (e)] and (18,3) [(c) and (f)] hyperbolic lattices in the presence of uniform [(a)-(c)] and inhomogeneous [(d)-(f)] magnetic flux. Red solid lines correspond to ρ with the field-induced charge-density-wave order for the nearest-neighbor Coulomb repulsion $V = 0.4 (\ll V_c)$. The total magnetic flux threading the system Φ_{total} is (a) 842, (b) 310, (c) 542, (d) 488, (e) 163 and (f) 281 in units of $\Phi_0/(2\pi)$. Insets depict formation of correlated insulators with a sharp spectral gap near zero energy for subcritical V via magnetic catalysis mechanism.

This outcome holds for uniform as well as bell-shaped inhomogeneous magnetic field, piercing the system. As external magnetic fields produce finite $\rho(0)$ [Fig. 2], a sizable condensation of the CDW order parameter (δ) takes place only in the large flux limit when $V \ll V_c$. Such an outcome can be appreciated from its BCS like scaling

$$\delta = a \exp(-b/[\Phi_{\text{total}} - \Phi_{\text{th}}]) \quad (5)$$

for $\Phi_{\text{total}} > \Phi_{\text{th}}$ and any fixed $V < V_c$, resulting from finite DOS near the zero energy [34]. Here a , b , and Φ_{th} are fitting parameters. For example, in the presence of uniform [inhomogeneous] magnetic fields $(a, b, \Phi_{\text{th}}) \approx (0.071, 70, 260)$ [(0.090, 175, 215)], (0.051, 17, 111) [(0.075, 70, 85)] and (0.050, 50, 180) [(0.050, 50, 180)] in the (10,3), (14,3) and (18,3) HDMs for $V = 0.55$, respectively. A nontrivial Φ_{th} purely stems from finite size effect for weak V . As the strength of subcritical V increases, δ becomes appreciable even for small Φ_{total} and Φ_{th} decreases monotonically. To unambiguously establish the magnetic catalysis mechanism on HDMs, we compute the difference between finite and zero magnetic field CDW order parameter, which for all choices of $V < V_c$ and for any Φ_{total} is a positive definite quantity. For $V > V_c$, δ is nonzero even in the absence of any magnetic field, which then increases as $\delta \sim \Phi_{\text{total}}^2$ in the small flux regime.

When δ is finite, HDMs become a correlated insulator at half-filling by spontaneously breaking the sublattice

exchange symmetry through the magnetic catalysis mechanism for $V < V_c$. To demonstrate this outcome we define a two-component superspinor $\Psi^T = (c_A, c_B)$, where c_A (c_B) is an N -dimensional spinor constituted by the annihilation operators on the sites of the A (B) sublattice. In this basis, the tight-binding Hamiltonian in the presence of magnetic fields and the Hamiltonian with the CDW order parameter takes the form

$$\hat{h}_0 = \begin{pmatrix} \mathbf{0} & \mathbf{t} \\ \mathbf{t}^\dagger & \mathbf{0} \end{pmatrix} \quad \text{and} \quad \hat{h}_{\text{CDW}} = \begin{pmatrix} \Delta & \mathbf{0} \\ \mathbf{0} & -\Delta \end{pmatrix}, \quad (6)$$

respectively, where $\mathbf{0}$ is an N -dimensional null matrix, \mathbf{t} and \mathbf{t}^\dagger are the intersublattice hopping matrices with the Peierls phase factors, and $\pm\Delta$ are N -dimensional diagonal matrices, whose entries are the self-consistent solutions of δ_A and δ_B at various sites of the system, respectively. As \hat{h}_0 and \hat{h}_{CDW} mutually *anticommute*, the CDW order acts like a mass for gapless fermions. Thus its spontaneous nucleation causes insulation near the half-filling, as shown in Fig. 4.

Summary and discussion. We show that the application of external uniform or inhomogeneous magnetic fields in HDMs, featuring a linearly vanishing DOS in the pristine condition, gives rise to a finite DOS near the zero energy which increases with the flux enclosed by the system. Then magnetic catalysis becomes operative in the entire HDM family through which a CDW

ordering nucleates even for subcritical NN Coulomb repulsion among (spinless) fermions. Inclusion of the spin degrees of freedom brings the on-site Hubbard repulsion onto the stage, conducive to the formation of an antiferromagnetic order if it is sufficiently strong [15]. When a magnetic field penetrates HDMs an easy-plane (perpendicular to the field direction) antiferromagnet, accompanied by a Zeeman coupling induced ferromagnetic order in the field direction is expected to emerge as the ground state for subcritical strength of Hubbard repulsion [19, 22]. A detailed study of this competition is left for a future investigation. It will also be fascinating to develop a field-theoretic description of this phenomenon in terms of the Gross-Neveu model [35] for Dirac fermions on curved space, subject to magnetic fields.

Designer electronic materials [36–39] and cold atomic setups [40–42] are two promising platforms where our predicted magnetic catalysis of CDW order in HDMs can be experimentally observed. A hyperbolic designer material can be created by growing its substrate on a suitable material with a different thermal expansion coefficient, such that under cooling a curved substrate is generated. It then can be decorated with the sites of the desired HDM. When placed in strong magnetic fields, designer HDMs can exhibit magnetic catalysis of dynamic mass generation. In cold atomic setups, hyperbolic tessellations can be achieved by suitable arrangements of the laser traps and magnetic fields can be introduced through the coupling of fermions with synthetic gauge fields [43, 44] to showcase magnetic catalysis.

Acknowledgments. B.R. was supported by a Startup grant from Lehigh University, and thanks Ariel Sommer, Abhisek Samanta and Sourav Manna for useful discussions.

* Corresponding author: bitan.roy@lehigh.edu

- [1] J. Zinn-Justin, *Quantum Field Theory and Critical Phenomena: Fifth Edition* (Oxford University Press, Oxford, UK, 2021).
- [2] I. F. Herbut, Interactions and Phase Transitions on Graphene’s Honeycomb Lattice, *Phys. Rev. Lett.* **97**, 146401 (2006).
- [3] I. F. Herbut, V. Juričić, and B. Roy, Theory of interacting electrons on the honeycomb lattice, *Phys. Rev. B* **79**, 085116 (2009).
- [4] B. Roy and S. Das Sarma, Quantum phases of interacting electrons in three-dimensional dirty Dirac semimetals, *Phys. Rev. B* **94**, 115137 (2016).
- [5] G. W. Semenoff, Condensed-Matter Simulation of a Three-Dimensional Anomaly, *Phys. Rev. Lett.* **53**, 2449 (1984).
- [6] I. Affleck and J. B. Marston, Large- n limit of the Heisenberg-Hubbard model: Implications for high- T_c superconductors, *Phys. Rev. B* **37**, 3774 (1988).
- [7] A. J. Kollár, M. Fitzpatrick, and A. A. Houck, Hyperbolic lattices in circuit quantum electrodynamics, *Nature* (London) **571**, 45 (2019).
- [8] J. Maciejko and S. Rayan, Hyperbolic band theory, *Sci. Adv.* **7**, eabe9170 (2021).
- [9] I. Boettcher, A. V. Gorshkov, A. J. Kollár, J. Maciejko, S. Rayan, and R. Thomale, Crystallography of hyperbolic lattices, *Phys. Rev. B* **105**, 125118 (2022).
- [10] N. Cheng, F. Serafin, J. McInerney, Z. Rocklin, K. Sun, and X. Mao, Band Theory and Boundary Modes of High-Dimensional Representations of Infinite Hyperbolic Lattices, *Phys. Rev. Lett.* **129**, 088002 (2022).
- [11] J. Maciejko and S. Rayan, Automorphic Bloch theorems for hyperbolic lattices, *Proc. Natl. Acad. Sci.* **119**, e2116869119 (2022).
- [12] A. Attar and I. Boettcher, Selberg trace formula in hyperbolic band theory, *Phys. Rev. E* **106**, 034114 (2022).
- [13] T. Bzdušek and J. Maciejko, Flat bands and band-touching from real-space topology in hyperbolic lattices, *Phys. Rev. B* **106**, 155146 (2022).
- [14] E. Kienzle and S. Rayan, Hyperbolic band theory through Higgs bundles, *Adv. Math.* **409**, 108664 (2022).
- [15] N. Glusceovich, A. Samanta, S. Manna, and B. Roy, Dynamic mass generation on two-dimensional electronic hyperbolic lattices, [arXiv:2302.04864](https://arxiv.org/abs/2302.04864).
- [16] V. P. Gusynin, V. A. Miransky, and I. A. Shovkovy, Catalysis of Dynamical Flavor Symmetry Breaking by a Magnetic Field in $2 + 1$ Dimensions, *Phys. Rev. Lett.* **73**, 3499 (1994).
- [17] G. Dunne and T. Hall, Inhomogeneous condensates in planar QED, *Phys. Rev. D* **53**, 2220 (1996).
- [18] V. P. Gusynin, V. A. Miransky, S. G. Sharapov, and I. A. Shovkovy, Excitonic gap, phase transition, and quantum Hall effect in graphene, *Phys. Rev. B* **74**, 195429 (2006).
- [19] I. F. Herbut, $SO(3)$ symmetry between Néel and ferromagnetic order parameters for graphene in a magnetic field, *Phys. Rev. B* **76**, 085432 (2007).
- [20] A. Raya and E. Reyes, Fermion condensate and vacuum current density induced by homogeneous and inhomogeneous magnetic fields in $(2 + 1)$ dimensions, *Phys. Rev. D* **82**, 016004 (2010).
- [21] B. Roy and I. F. Herbut, Inhomogeneous magnetic catalysis on graphene’s honeycomb lattice, *Phys. Rev. B* **83**, 195422 (2011).
- [22] B. Roy, M. P. Kennett, and S. Das Sarma, Chiral symmetry breaking and the quantum Hall effect in monolayer graphene, *Phys. Rev. B* **90**, 201409 (2014).
- [23] R. Peierls, Zur Theorie des Diamagnetismus von Leitungselektronen, *Z. Physik* **80**, 763 (1933).
- [24] A. Comtet and P. J. Houston, Effective action on the hyperbolic plane in a constant external field, *J. Math. Phys. (N.Y.)* **26**, 185 (1985).
- [25] M. Ludewig and G. C. Thiang, Gaplessness of Landau Hamiltonians on Hyperbolic Half-planes via Coarse Geometry, *Commun. Math. Phys.* **386**, 87 (2021).
- [26] K. Ikeda, S. Aoki, and Y. Matsuki, Hyperbolic band theory under magnetic field and Dirac cones on a higher genus surface, *J. Phys.: Condens. Matter* **33**, 485602 (2021).
- [27] A. Stegmaier, L. K. Upreti, R. Thomale, and I. Boettcher, Universality of Hofstadter Butterflies on Hyperbolic Lattices, *Phys. Rev. Lett.* **128**, 166402 (2022).
- [28] R. Mosseri, R. Vogeler, and J. Vidal, Aharonov-Bohm cages, flat bands, and gap labeling in hyperbolic tilings, *Phys. Rev. B* **106**, 155120 (2022).

- [29] Y. Aharonov and A. Casher, Ground state of a spin- $\frac{1}{2}$ charged particle in a two-dimensional magnetic field, *Phys. Rev. A* **19**, 2461 (1979).
- [30] Y. Inahama and S.-I. Shirai, Spectral properties of Pauli operators on the Poincaré upper-half plane, *J. Math. Phys. (N.Y.)* **44**, 2451 (2003).
- [31] T. Mine and Y. Nomura, Landau levels on the hyperbolic plane in the presence of Aharonov–Bohm fields, *J. Funct. Anal.* **263**, 1701 (2012).
- [32] B. Roy and J. D. Sau, Competing charge-density wave, magnetic, and topological ground states at and near Dirac points in graphene in axial magnetic fields, *Phys. Rev. B* **90**, 075427 (2014).
- [33] B. Roy, Interacting nodal-line semimetal: Proximity effect and spontaneous symmetry breaking, *Phys. Rev. B* **96**, 041113 (2017).
- [34] B. Roy and J. D. Sau, Magnetic catalysis and axionic charge density wave in Weyl semimetals, *Phys. Rev. B* **92**, 125141 (2015).
- [35] D. J. Gross and A. Neveu, Dynamical symmetry breaking in asymptotically free field theories, *Phys. Rev. D* **10**, 3235 (1974).
- [36] K. K. Gomes, W. Mar, W. Ko, F. Guinea, and H. C. Manoharan, Designer Dirac fermions and topological phases in molecular graphene, *Nature (London)* **483**, 306 (2012).
- [37] M. Polini, F. Guinea, M. Lewenstein, H. C. Manoharan, and V. Pellegrini, Artificial honeycomb lattices for electrons, atoms and photons, *Nature Nanotech* **8**, 625 (2013).
- [38] L. C. Collins, T. G. Witte, R. Silverman, D. B. Green, and K. K. Gomes, Imaging quasiperiodic electronic states in a synthetic Penrose tiling, *Nat. Commun.* **8**, 15961 (2017).
- [39] S. N. Kempkes, M. R. Slot, S. E. Freeney, S. J. M. Zevenhuizen, D. Vanmaekelbergh, I. Swart, and C. M. Smith, Design and characterization of electrons in a fractal geometry, *Nat. Phys.* **15**, 127 (2019).
- [40] T. Esslinger, Fermi-Hubbard Physics with Atoms in an Optical Lattice, *Annu. Rev. Condens. Matter Phys.* **1**, 129 (2010).
- [41] L. W. Cheuk, M. A. Nichols, K. R. Lawrence, M. Okan, H. Zhang, E. Khatami, N. Trivedi, T. Paiva, M. Rigol, and M. W. Zwierlein, Observation of spatial charge and spin correlations in the 2D Fermi-Hubbard model, *Science* **353**, 1260 (2016).
- [42] A. Mazurenko, C. S. Chiu, G. Ji, P. M. F., M. Kanász-Nagy, R. Schmidt, F. Grusdt, E. Demler, D. Greif, and M. Greiner, A cold-atom Fermi-Hubbard antiferromagnet, *Nature (London)* **545**, 462 (2017).
- [43] M. Aidelsburger, M. Atala, M. Lohse, J. T. Barreiro, B. Paredes, and I. Bloch, Realization of the Hofstadter Hamiltonian with Ultracold Atoms in Optical Lattices, *Phys. Rev. Lett.* **111**, 185301 (2013).
- [44] M. Aidelsburger, Artificial gauge fields and topology with ultracold atoms in optical lattices, *J. Phys. B: At. Mol. Opt. Phys.* **51**, 193001 (2018).